Free-Space Excitation of Propagating Surface Plasmon Polaritons by Nonlinear Four-Wave Mixing

Jan Renger,[1] Romain Quidant,[1] Niek van Hulst,[1] Stefano Palomba,[2] and Lukas Novotny[1,2]
[1]*ICFO-Institut de Ciencies Fotoniques, Mediterranean Technology Park, 08860 Castelldefels (Barcelona), Spain*
[2]*Institute of Optics, University of Rochester, Rochester, New York 14627, USA*
(Received 25 August 2009; revised manuscript received 25 November 2009; published 21 December 2009)

A unique feature of surface plasmon polaritons (SPPs) is that their in-plane momentum is larger than the momentum of free-propagating photons of the same energy. Therefore, it is believed that they can be excited only by evanescent fields created by total internal reflection or by local scattering. Here, we provide the first demonstration of free-space excitation of surface plasmons by means of nonlinear four-wave mixing. The process involves the vectorial addition of the momenta of three incident photons, making it possible to penetrate the light cone and directly couple to the SPP dispersion curve. Using this technique, surface plasmons can be launched on any metal surface by simply overlapping two beams of laser pulses incident from resonant directions. The excitation scheme is also applicable to other bound modes, such as waveguide modes, surface phonon polaritons, and excitations of 2D electron gases.

DOI: 10.1103/PhysRevLett.103.266802 PACS numbers: 73.20.Mf, 42.65.Ky, 78.47.nj, 78.68.+m

Surface plasmon polaritons (SPPs) are electromagnetic excitations bound to a metal's surface. Because of their strong localization and resonant properties they find application in biosensing [1], optoelectronics [2,3], metamaterials [4], enhanced optical transmission through nanoapertures [5], super-resolution imaging [6], and negative refraction [7]. The electromagnetic field of a surface plasmon polariton (SPP) is confined to the surface of a metal and decays exponentially away from the surface. For a metal-air interface the wave vector parallel to the interface obeys the dispersion relation

$$k_{\mathrm{spp}}(\omega) = \frac{\omega}{c}\sqrt{\frac{\varepsilon(\omega)}{\varepsilon(\omega)+1}}, \tag{1}$$

where ω is the angular frequency, c the vacuum speed of light, and ε the dielectric function of the metal. As shown by the red curve in Fig. 1, the dispersion relation lies to the right of the light cone defined by $k = \omega/c$ (shaded area) and hence cannot be excited by a single free-propagating photon. Therefore, various alternative excitation schemes have been developed over the years, which either rely on coupling via evanescent waves, such as the Kretschmann-Raether configuration [8] and the Otto [9] configuration, or on gratings and defects [10,11] at the metal surface in order to bridge the momentum gap between the SPP and the incident radiation. However, these processes inevitably lead to increased losses (due to finite film thickness), leakage radiation or scattering, which reduces the SPP propagation length and increases background radiation [12]. In this work, we overcome these restrictions and provide the first demonstration of direct SPP excitation on flat surfaces of *bulk* metals by free-propagating radiation. Our approach allows SPPs to be launched on any planar metal surface by nonlinear mixing of photons from two separate laser beams.

The multiphoton excitation scheme introduced here can be readily understood on the basis of energy and momentum conservation. As illustrated in Fig. 1, the process employs three photons, each of them propagating within the light cone of free radiation. These photons are generated by two coherent incident laser beams with frequencies ω_1 and ω_2 incident from angles Θ_1 and Θ_2, respectively. The angles are measured from the surface normal ($\mathbf{n}_\perp$) in

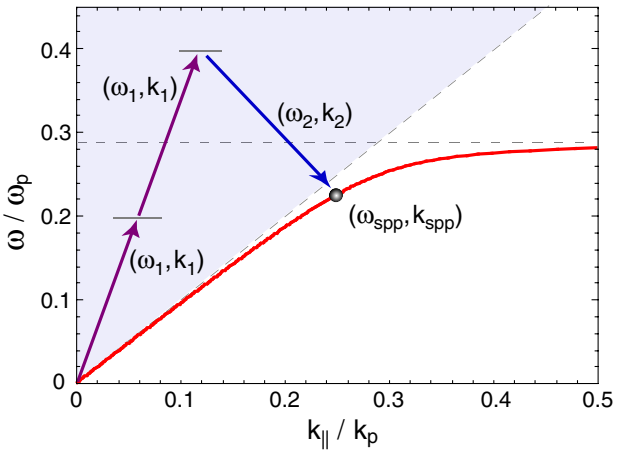

FIG. 1 (color online). Principle of surface plasmon excitation by nonlinear four-wave mixing. The SPP dispersion curve $k_{\mathrm{spp}}(\omega)$ (solid line) is located to the right of the light cone (shaded area) prohibiting the excitation by a single free-propagating photon. The vectorial summation of three incident photons, all contained within the light cone, makes it possible to penetrate the light cone and to couple to the SPP dispersion curve. The axes are normalized by the plasma frequency ω_p and corresponding wave vector $k_p = \omega_p/c$. For gold: $\hbar\omega_p \sim 9$ eV.

clockwise direction. The two beams induce nonlinear polarizations $\mathbf{P}^{(3)}$ at frequencies:

$$\omega_{\mathrm{spp}_1} = 2\omega_1 - \omega_2, \qquad \omega_{\mathrm{spp}_2} = 2\omega_2 - \omega_1. \tag{2}$$

In each of these processes one beam contributes two photons whereas the other contributes a single photon. Momentum conservation requires that the wave vectors of the excited SPPs are equal to the total in-plane wave vector $\mathbf{k}_\parallel$ of the three incident photons ($\mathbf{k}_\parallel \cdot \mathbf{n}_\perp = 0$). In terms of the incident angles we obtain

$$\begin{aligned} \mp \mathrm{Re}\{k_{\mathrm{spp}}(\omega_{\mathrm{spp}_1})\} &= 2k_1 \sin\Theta_1 - k_2 \sin\Theta_2, \\ \pm \mathrm{Re}\{k_{\mathrm{spp}}(\omega_{\mathrm{spp}_2})\} &= 2k_2 \sin\Theta_2 - k_1 \sin\Theta_1, \end{aligned} \tag{3}$$

where $k_1 = \omega_1/c$, $k_2 = \omega_2/c$. The upper signs of k_{spp} correspond to solutions $\Theta_2 > \Theta_1$, and the lower signs to $\Theta_2 < \Theta_1$. After combining Eqs. (1)–(3) it becomes evident, that momentum conservation can only be fulfilled for certain values of Θ_1 and Θ_2. However, within the angular regions for which solutions exist, the momentum of the excited plasmon can be tuned by adjusting the incident angles of the excitation beams.

Using the dielectric function $\varepsilon(\omega)$ for gold [13] and the excitation wavelengths $\lambda_1 = 707$ nm and $\lambda_2 = 800$ nm, Eqs. (1)–(3) yield the curves shown in Fig. 2. The circles in Fig. 2 indicate the locations that correspond to a relative angle between excitation beams of $\Theta_2 - \Theta_1 = 60°$, as used in our measurements. They are calculated as

$$\begin{aligned} [\Theta_1, \Theta_2] &= [-16.0°, 44.0°] \quad \text{for } \lambda_{\mathrm{spp}_1} = 633 \text{ nm}, \\ [\Theta_1, \Theta_2] &= [-63.9°, -3.9°] \quad \text{for } \lambda_{\mathrm{spp}_2} = 921 \text{ nm}. \end{aligned} \tag{4}$$

In our experiments we use a Ti:sapphire laser providing pulses of duration ~200 fs and center wavelength $\lambda_2 = 800$ nm, and an optical parametric oscillator (OPO) providing pulses of similar duration and wavelength $\lambda_1 = 707$ nm. The beams are first expanded to 10 mm diameter and then focused by two lenses of focal length $f = 50$ mm on a gold surface with surface roughness of 2.3 $\mathrm{nm_{rms}}$, as determined by atomic force microscopy. The spot diameters at the surface are ~4.5 μm and are spatially overlapping. By use of a delay line, the laser pulses are also made to overlap in time. In the experiments, the angle between the two excitation beams is held fixed at $\Theta_2 - \Theta_1 = 60°$.

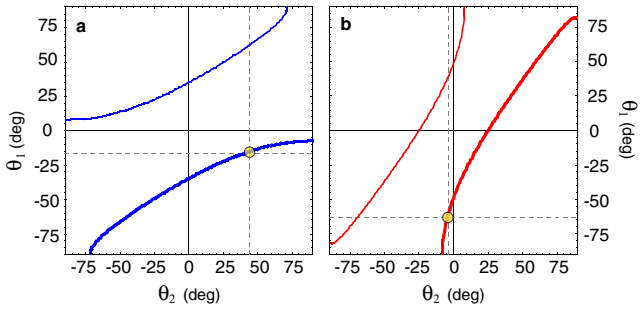

FIG. 2 (color online). Excitation angles Θ_1 and Θ_2 required for surface plasmon excitation. The upper branches (thin lines) are for $\Theta_2 < \Theta_1$ and the lower branches (thick lines) for $\Theta_2 > \Theta_1$. The excitation frequencies are combined as (a) $\omega_{\mathrm{spp}_1} = 2\omega_1 - \omega_2$ ($\lambda_{\mathrm{spp}_1} = 633$ nm) and (b) $\omega_{\mathrm{spp}_2} = 2\omega_2 - \omega_1$ ($\lambda_{\mathrm{spp}_2} = 921$ nm). The curves follow from the dielectric function $\varepsilon(\omega)$ for gold and the excitation wavelengths $\lambda_1 = 707$ nm and $\lambda_2 = 800$ nm. The circles indicate the solutions for the relative angle $\Theta_2 - \Theta_1 = 60°$ used in the experiments.

Because the excited SPPs are confined to the gold surface it is not possible to directly image their propagation. Therefore, as shown in Figs. 3(a) and 3(c), we have fabricated gratings into the gold surface to convert the SPPs into propagating radiation. The gratings consist of periodic grooves of depth 70 nm and width 150 nm, produced by electron beam lithography and reactive ion etching. For λ_{spp_1} we use a period of 700 nm and for λ_{spp_2} a period of 535 nm. It has to be emphasized that the excitation beams do not interact with the gratings; i.e., the excitation spots are sufficiently displaced from the gratings. The outcoupled radiation is collected by $f = 50$ nm lenses, filtered by optical stop-band filters to reject light at the incident frequencies, and then sent into a fiber-coupled spectrometer. Alternatively, the collected light is filtered by narrow-band bandpass filters centered at λ_{spp_1} and λ_{spp_2} and detected with a single-photon counting avalanche photodiode.

To experimentally verify the predictions in (4), we displace the excitation beams from the gratings and record the intensities of the outcoupled surface plasmons as a function of sample rotation angle, which is calibrated against Θ_2. For excitation pulses that are not overlapping in time and space we observe no surface plasmon excitation. On the other hand, when spatial and temporal overlap is ensured and when the resonance conditions are met, we readily detect radiation due to surface plasmon excitation [cf. Figs. 3(b) and 3(d)]. The peak positions for Θ_2 are in excellent agreement with the theoretical predictions in (4). Slight deviations are due to calibration uncertainties and the angular dependence of the detection efficiency. The width of the peaks $\Delta\Theta_1 \approx 4°$ originates from the fact that our excitation beams are not plane waves but focused beams with an angular range defined by the focusing lenses, the beam waist of the incident beams, and the dielectric function $\varepsilon(\omega)$ of gold.

The direction of SPP propagation is defined by the excitation angles Θ_1 and Θ_2 (cf. Fig. 2). Therefore, the excitation spots need to be placed on the "entrance" side of the gratings. We observe no surface plasmon excitation when the excitation spots are placed on the opposite side of the gratings, which verifies the SPP propagation directions illustrated in Figs. 3(a) and 3(c). Notice the apparent backwards propagation of the SPP at $\lambda_{\mathrm{spp}_2} = 921$ nm. This nonintuitive scenario arises because for this process the momentum of photons with energy $\hbar\omega_1$ is *subtracted* from

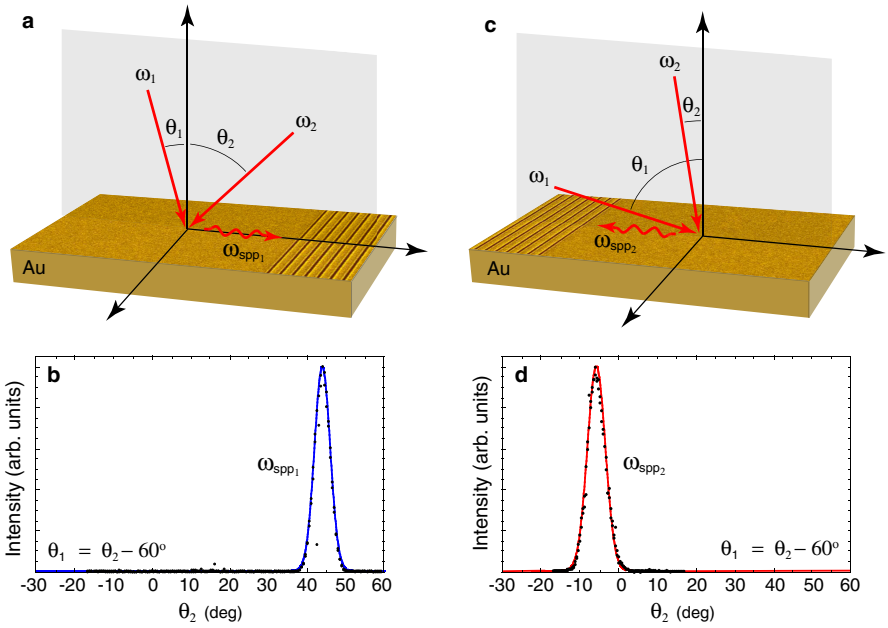

FIG. 3 (color online). (a, c) Experimental configuration with overlaid scanning electron microscope images of the sample surface showing the gratings used for SPP outcoupling. The figures illustrate the resonant incident angles (arrows) and the direction of SPP propagation (wavy lines). (a) Configuration for plasmon $\lambda_{\mathrm{spp}_1} = 633$ nm excited by $\omega_{\mathrm{spp}_1} = 2\omega_1 - \omega_2$. (c) Configuration for plasmon $\lambda_{\mathrm{spp}_2} = 921$ nm excited by $\omega_{\mathrm{spp}_2} = 2\omega_2 - \omega_1$. (b, d) Experimental results showing the intensity of the outcoupled surface plasmons as a function of excitation angle Θ_2 using $\Theta_1 = \Theta_2 - 60°$. Black dots are data and the solid curves are Gaussian fitting functions. The peak positions agree with the theoretical predictions in Eq. (4).

the momentum of photons with energy $\hbar\omega_2$, giving rise to a negative sign.

We have also measured the dependence of the plasmon intensity on the power of the excitation beams (data not shown) and verified that plasmon excitation depends quadratically on the excitation power if the process involves two photons from the same beam, and linearly if it involves only a single photon. In Fig. 4 we show the dependence of the detected SPP intensity on the polarization of the exciting laser beams. (a, b) refer to the SPP at wavelength $\lambda_{\mathrm{spp}_1} = 633$ nm, and (c, d) to the SPP at wavelength $\lambda_{\mathrm{spp}_2} = 921$ nm. The polarization angle $\Phi = 0°$ specifies s-polarized incidence; i.e., the electric vector is parallel to the gold surface. On the other hand, p-polarized incidence corresponds to a polarization angle $\Phi = \pi/2$. While the polarization of one of the incident beams is varied the polarization of the other beam is held fixed at $\Phi = \pi/2$ (p polarization). The data in Fig. 4 indicate that the data points follow predominantly a $\sin^2\Phi$ and a $\sin^4\Phi$ dependence. This behavior is consistent with a linear and quadratic power dependence: for a field $\mathbf{E}$ varying as $\sin\Phi$ a linear power dependence renders a signal varying as $\sin^2\Phi$, whereas a quadratic power dependence yields a signal varying as $\sin^4\Phi$. If both of the incident beams are s polarized we observe no SPP excitation. Furthermore, we verified that the outcoupled SPP radiation is purely p polarized. Interestingly, we observe an additional signal variation in the valleys of the curve shown in Fig. 4(d), which can be explained if two independent components of the susceptibility tensor $\chi^{(3)}(\omega_{\mathrm{spp}_2}; \omega_2, \omega_2, -\omega_1)$ are taken into account. A detailed analysis will be presented elsewhere. The SPP intensity was also recorded as a function of the separation between excitation spot and the grating used for outcoupling (data not shown). The data agrees well with the theoretical decay curves characterized by the single-surface decay lengths $L_{633} = 10.2$ μm and $L_{921} = 78$ μm, respectively.

For typical excitation peak intensities of $\hat{I}_1 = 22$ GW/cm^2 and $\hat{I}_2 = 46$ GW/cm^2 we determine a SPP excitation rate of 10^8 plasmons per second, which corresponds to a peak intensity of $\hat{I}_{\mathrm{spp}} \sim 12$ W/cm^2. This value can be improved by several orders of magnitude by using higher intensities, excitation frequencies near the surface plasmon resonance (~ 510 nm for a planar gold surface) [14], and coherent control [15]. It is important to emphasize that the plasmons excited by four-wave mixing have a well-defined energy, momentum, and directivity, which is not the case for free-electron impact [16,17].

The multiphoton excitation scheme described in this work allows surface plasmons to be excited anywhere on a metal surface. The energy and momentum of the excited plasmons can be selected by proper choice of laser energies and excitation angles. The process makes use of vectorial photon momentum summation and does not rely on thin films, gratings, or scattering centers. For example, the method does not require coupling prisms and allows

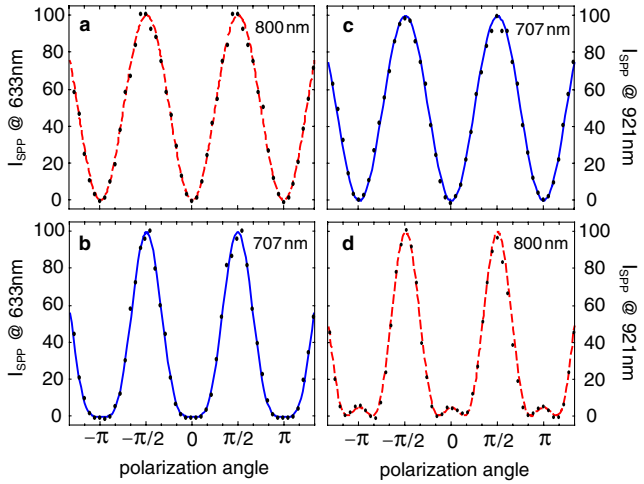

FIG. 4 (color online). Dependence of the SPP intensity on the polarization of the excitation beams. $\Phi = 0°$ corresponds to s polarization and $\Phi = \pi/2$ to p polarization. (a),(b) refer to the SPP at wavelength $\lambda_{spp_1} = 633$ nm, and (c),(d) to the SPP at wavelength $\lambda_{spp_2} = 921$ nm. The numbers in the figure indicate the wavelength of the laser whose polarization is being varied. The polarization of the other laser beam is held constant at $\Phi = \pi/2$ (p polarization). Black dots are data and solid lines are theoretical curves.

SPPs to be excited in confined areas, such as in vacuum chambers, ovens, or cryostats. At the resonant angles and at the nonlinear frequency ω_{spp} *only* SPPs are excited and there is no scattered radiation of the same frequency. In an extension of the work described here, it is conceivable to excite SPPs with radially polarized annular beams [18] thereby providing the possibility of generating converging or diverging plasmon fields. The work described here can also be extended to configurations using multiple SPP excitation spots, for example, by use of zone plates or diffractive optics. Surface plasmons excited at different locations are then able to interfere with each other, which can be exploited for plasmon focusing, guiding and control [10]. By introducing time delays between different excitation regions it will be possible to implement coherent control of surface plasmon propagation [15,19], opening up possibilities for SPP amplification and SPP based logic [3].

The method of vectorially adding different photon momenta can also be employed for the excitation of other planar modes, such as surface phonon polaritons [20], waveguide modes, surface exciton polaritons [21], and modes associated with two-dimensional electron gases (2DEG), such as magnetoplasmons and magnetorotons [22]. Multiphoton excitation makes it possible to bypass the limitations of reciprocity [23] and to excite nonradiative (dark) modes radiatively.

This research was funded by the U.S. Department of Energy (DE-FG02-01ER15204), the Catalan AGAUR pivprogram, and ICREA. We thank Mark Kreuzer and Michael Yarrow (Radiantis) for technical support.

[1] J. Homola, in *Frontiers in Planar Lightwave Circuit Technology*, NATO Science Series II: Mathematics, Physics, and Chemistry Vol. 216 (Kluwer, Dordrecht, 2006), p. 101.
[2] D. Pacifici, H. J. Lezec, and H. A. Atwater, Nat. Photon. **1**, 402 (2007).
[3] K. F. MacDonald, Z. L. Samson, M. I. Stockman, and N. I. Zheludev, Nat. Photon. **3**, 55 (2009).
[4] N. Liu *et al.*, Nature Mater. **7**, 31 (2008).
[5] T. W. Ebbesen *et al.*, Nature (London) **391**, 667 (1998).
[6] N. Fang, H. Lee, C. Sun, and X. Zhang, Science **308**, 534 (2005).
[7] J. Valentine *et al.*, Nature (London) **455**, 376 (2008).
[8] E. Kretschmann and H. Raether, Z. Naturforsch. A **23a**, 2135 (1968).
[9] A. Otto, Z. Phys. **216**, 398 (1968).
[10] F. Lopez-Tejeira *et al.*, Nature Phys. **3**, 324 (2007).
[11] J. Renger, S. Grafström, and L. M. Eng, Phys. Rev. B **76**, 045431 (2007).
[12] A. Drezet *et al.*, Mater. Sci. Eng. B **149**, 220 (2008).
[13] P. B. Johnson and R. W. Christy, Phys. Rev. B **6**, 4370 (1972).
[14] H. B. Liao *et al.*, Opt. Lett. **23**, 388 (1998).
[15] M. Aeschlimann *et al.*, Nature (London) **446**, 301 (2007).
[16] M. V. Bashevoy *et al.*, Nano Lett. **6**, 1113 (2006).
[17] W. Cai, R. Sainidou, J. Xu, A. Polman, and F. J. G. de Abajo, Nano Lett. **9**, 1176 (2009).
[18] L. Novotny, M. R. Beversluis, K. S. Youngworth, and T. G. Brown, Phys. Rev. Lett. **86**, 5251 (2001).
[19] M. I. Stockman, S. V. Faleev, and D. J. Bergman, Appl. Phys. B **74**, s63 (2002).
[20] R. Hillenbrand and F. Keilmann, Appl. Phys. Lett. **80**, 25 (2002).
[21] F. D. De Martini *et al.*, Phys. Rev. Lett. **38**, 1223 (1977).
[22] I. V. Kukushkin *et al.*, Science **324**, 1044 (2009).
[23] R. Carminati, M. Nieto-Vesperinas, and J.-J. Greffet, J. Opt. Soc. Am. A **15**, 706 (1998).